Journal of Applied Electrochemistry **31**: 373–378, 2001.

Platinum-based alloys as oxygen–reduction catalysts for solid–polymer–electrolyte direct methanol fuel cells

M. NEERGAT[1], A.K. SHUKLA[1]* and K.S. GANDHI[2]
[1]*Solid State and Structural Chemistry Unit*
[2]*Department of Chemical Engineering, Indian Institute of Science, Bangalore-560012, India*
*(*author for correspondence, fax: +91-80-3601310; e-mail: shukla@sscu.iisc.ernet.in)*

Received 8 February 2000; accepted in revised form 30 October 2000

Key words: alloy catalysts, direct methanol fuel cells, oxygen–reduction reaction

Abstract

Electrocatalytic activities of various carbon-supported platinum-based binary, namely, Pt–Co/C, Pt–Cr/C and Pt–Ni/C, and ternary, namely, Pt–Co–Cr/C and Pt–Co–Ni/C, alloy catalysts towards oxygen reduction in solid–polymer–electrolyte direct methanol fuel cells were investigated at 70 °C and 90 °C both at ambient and 2 bar oxygen pressures. It was found that Pt–Co/C exhibits superior activity relative to Pt/C and other alloy catalysts.

1. Introduction

At present, platinum is being used as oxygen–reduction catalyst in solid–polymer–electrolyte direct methanol fuel cells (SPE–DMFCs) [1–7]. But Nafion, the most commonly employed solid–polymer–electrolyte membrane, has the drawback of permeability to methanol which poisons the platinum catalyst [1–3]. Attempts are therefore being made to find methanol-tolerant oxygen–reduction catalysts for SPE–DMFCs [8, 9]. Several carbon-supported binary and ternary-alloys of platinum, namely, Pt–Ni/C and Pt–Co–Ni/C, have been shown to offer good performance as oxygen–reduction catalysts in phosphoric acid fuel cells (PAFCs) [10–21] and more recently in polymer electrolyte fuel cells (PEFCs) [22–24] but the viability of these alloy catalysts as oxygen–reduction catalysts in SPE–DMFCs has not been tested hitherto. In this communication, we report the electrochemical activities of several carbon-supported platinum-based binary and ternary-alloy catalysts, namely, Pt–Ni/C, Pt–Co/C, Pt–Cr/C, Pt–Co–Cr/C and Pt–Co–Ni/C, towards oxygen reduction in SPE–DMFCs in relation to Pt/C catalyst. It is found that among the catalysts studied, Pt-Co/C exhibits superior performance towards oxygen reduction.

2. Experimental details

2.1. *Catalyst preparation and their physical characterization*

The various carbon-supported platinum-based binary and ternary alloy catalysts prepared during this study, besides Pt/C, were Pt–Co/C, Pt–Cr/C, Pt–Ni/C, Pt–Co–Cr/C, and Pt–Co–Ni/C.

2.1.1. *Preparation of 20 wt % Pt/Vulcan XC-72*

20 wt % platinized carbon was prepared by the sulfito-complex route [2, 21]. For this purpose, $Na_6[Pt(SO_3)_4]$ precursor was obtained from chloroplatinic acid. Chloroplatinic acid was dissolved in distilled water and the pH of the solution was adjusted to 7 by adding Na_2CO_3. Subsequently, the pH of the solution was lowered to 3 by adding $NaHSO_3$. The solution was then gently warmed until it became colourless. The pH of the solution was then raised to 6 by adding Na_2CO_3. This resulted in a white precipitate of $Na_6[Pt(SO_3)_4]$ which was filtered, washed copiously with hot distilled water, and dried in an air oven at 80 °C.

To obtain 20 wt % Pt/Vulcan XC-72 catalyst sample, the required amount of Vulcan XC-72 was suspended in distilled water and agitated in an ultrasonic water bath at about 80 °C to form the slurry. The required amount of $Na_6[Pt(SO_3)_4]$ was dissolved in 1 M H_2SO_4 and diluted with distilled water. This solution was added dropwise to the carbon slurry with constant stirring at 80 °C. This was followed by the addition of 30% H_2O_2 with the temperature maintained at 80 °C which resulted in vigorous gas evolution; the solution was further stirred for 1 h. Subsequently, platinized carbon was obtained by reducing it with 1 wt % formic acid solution which was filtered, washed copiously with hot distilled water and dried in an air oven at 80 °C for 2 h.

2.1.2. *Preparation of binary Pt–Co/C, Pt–Cr/C, and Pt–Ni/C alloy catalysts*

The required amount of 16 wt % Pt/Vulcan XC-72 was prepared as described in Section 2.1.1 and dispersed in

distilled water followed by ultrasonic blending for 15 min. The pH of the solution was raised to 8 with dilute ammonium hydroxide. Stirring was continued during and after the pH adjustment. The required amount of respective salt solution ($Co(NO_3)_2$ or $Ni(NO_3)_2$ or $Cr(NO_3)_3$) containing the required amount of the salt was added to this solution. This was followed by the addition of dilute HCl to the solution until a pH of 5.5 was attained. Stirring was continued for 1 h and then the resultant mass was dried at 90 °C in an air oven for 2 h. Subsequently, it was ground well and the powder was heat-treated at 900 °C in nitrogen atmosphere for 1 h to form the respective binary alloy catalyst. The catalyst compositions were maintained as 20 wt % Pt–Co/C, 20 wt % Pt–Cr/C, and 20 wt % Pt–Ni/C.

2.1.3. *Preparation of ternary Pt–Co–Cr/C and Pt–Co–Ni/C alloy catalysts*

The required amount of 16 wt % Pt/Vulcan XC-72 was prepared as described in Section 2.1.1 and dispersed in distilled water followed by ultrasonic blending for 15 min. The pH of the solution was adjusted to 8 with dilute NH_4OH solution. Stirring was continued during and after the pH adjustment. The required amount of the $Cr(NO_3)_3$ salt solution of known concentration was added to the pH adjusted solution and its pH was re-adjusted to 5.5 by addition of dilute HCl. A solution of $Co(NO_3)_2$ of known concentration containing the required amount of cobalt was then added to this solution. The pH was maintained at 5.5 by adding dilute HCl. Stirring was continued during the process. The solution was dried at about 90 °C and then heat-treated at 900 °C in nitrogen atmosphere for 1 h. Pt–Co–Cr/Vulcan XC-72 catalyst thus obtained was characterized by obtaining its powder X-ray diffraction pattern. The catalyst composition was maintained as 20 wt % Pt–Co–Cr/C. A similar procedure was adopted to prepare Pt–Co–Ni/Vulcan XC-72 catalyst.

All the carbon-supported platinum-based binary and ternary catalysts were characterized by recording their powder X-ray diffraction (XRD) patterns on a Philips X -Pert 3710 X-ray diffractometer using CuK_α radiation. The catalysts were also subjected to energy dispersive analysis by X-rays (EDAX) employing a Jeol JSM-840A scanning electron microscope to determine the composition of the elements.

2.2. *Preparation of membrane electrode assemblies (MEAs)*

Both the anode and cathode consist of a backing layer, a gas-diffusion layer and a reaction layer. A Teflonized (20 wt % Teflon) carbon paper (Kureha) of 0.3 mm thickness was employed as the backing layer in these electrodes. To prepare the gas-diffusion layer, Ketjen Black carbon was suspended in water and agitated in an ultrasonic water bath. To this, 10 wt % of Teflon (Fluon GP-2) suspension was added with continuous agitation. The required amount of cyclohexane was then added to it dropwise. The resultant slurry was spread on a Teflonized carbon paper and dried in an air oven at 80 °C for 2 h. To prepare the reaction layer, the required amount of the catalyst (20 wt % Pt/C or carbon-supported Pt-based alloys for the cathode or Pt–Ru/C for the anode) was mixed with 10 wt % of Teflon suspension. The mixture was suspended in water and agitated in an ultrasonic water bath, and 15 wt % of Nafion (5 wt %) solution (Aldrich) was added to it with continuous stirring. The paste thus obtained was spread onto the gas-diffusion layer of the electrode, and pressed at 75 kg cm^{-2} for 5 min. The anode contained Pt–Ru/C catalyst with a platinum loading of 4 mg cm^{-2} which was kept identical in all the MEAs. The platinum content of the cathode in all the MEAs was maintained at 1 mg cm^{-2}. A thin layer of 5 wt % Nafion solution was spread on the surface of each electrode. The membrane electrode assembly was obtained by pressing the cathode and anode on either side of a pre-treated Nafion-117 proton exchange membrane by compaction with a pressure of 50 kg cm^{-2} at 127 °C for 3 min.

2.3. *Electrochemical studies*

Liquid-feed SPE–DMFCs were assembled employing the membrane electrode assemblies described in Section 2.2. The anode and cathode of the SPE–DMFCs were contacted at their rear with gas/fluid-flow field plates machined from high-density graphite blocks in which channels had been formed. The channels were machined to achieve minimum mass-polarization in the SPE–DMFCs. The ridges between the channels make electrical contact with the back of the electrode and conduct the current to the external circuit. The channels supply methanol to the anode and oxygen to the cathode. Electrical heaters were placed behind each of the graphite blocks in order to heat the cell to the desired temperature. The methanol solution was pumped to the anode chamber through a peristaltic pump and the unreacted solution was collected in the reservoir. Oxygen gas at about 2 bar pressure was introduced to the cathode chamber. The graphite blocks were also provided with collectors for electrical contact and small holes to accommodate thermocouples. An electrolytic cell was prepared by coupling two palladium–gold grids (5 mm × 10mm) onto the Nafion membrane. A small d.c. voltage was imposed between these electrodes. The cathode, where hydrogen is generated, was used as a reference electrode after calibrating it against a bubbling hydrogen electrode by adjusting the current through the electrolytic cell so as to give a potential difference of ~1 mV between the cathode and the bubbling hydrogen electrode. The cathode was used as reference electrode and is referred as dynamic hydrogen electrode (DHE). Galvanostatic-polarization data on the activated SPE–DMFCs were obtained at various pressures and temperatures. The active geometrical area of the electrodes was 4 cm^2. The current densities were calculated from the active geometric area of the electrodes. *In situ*

cyclic voltammetric studies on electrodes with different electrocatalysts were conducted to obtain platinum surface areas employing an Autolab (AUT-30) potentiostat/Galvanostat. Electrochemical surface areas of the electrodes from the voltammetric data were estimated using the procedure described in the literature [25].

3. Results and discussion

The powder X-ray diffraction (XRD) patterns of various carbon-supported binary and ternary alloy catalysts are given in Figures 1 and 2, respectively. The diffraction peak at $2\theta \sim 25°$ observed in all the diffraction patterns of the carbon-supported catalysts is due to the (002) plane of the hexagonal structure of Vulcan XC-72 carbon. Although the XRD patterns of carbon-supported Pt–Ni and Pt–Cr catalysts resemble the face-centred cubic structure of carbon-supported Pt catalyst, these actually belong to the single-phase of disordered Pt–Ni and Pt–Cr alloys [13]. By contrast, the XRD patterns of carbon-supported Pt–Co catalyst resemble the ordered tetragonal structure of Pt–Co alloy [13]. The XRD patterns of the carbon-supported ternary Pt–Co–Cr and Pt–Co–Ni alloy catalysts are akin to the ordered tetragonal structure reported for single-phase alloys [26, 27]. The EDAX analysis of all the electrocatalysts along with their nominal compositions are given in Table 1. The EDAX analysis of binary-alloy catalysts gave near 1:1 atomic ratio of Pt : base metal (M) ratio and physical characterization of these alloy catalysts suggest these to

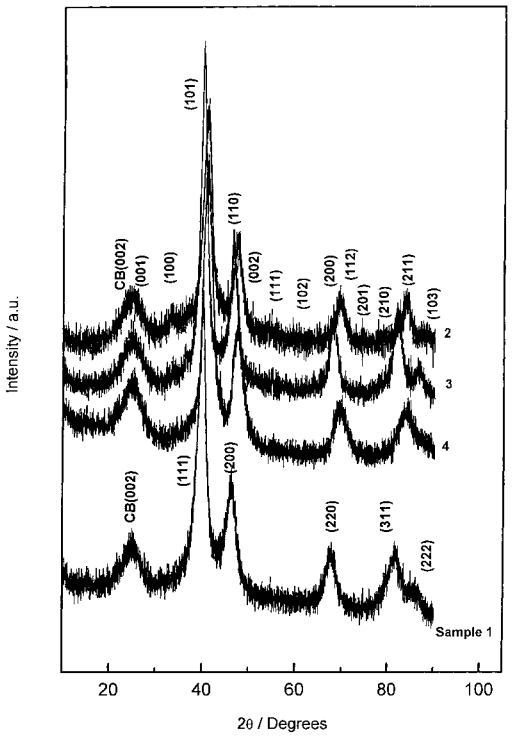

Fig. 1. Powder X-ray diffraction patterns of carbon-supported platinum-based binary-alloy catalysts.

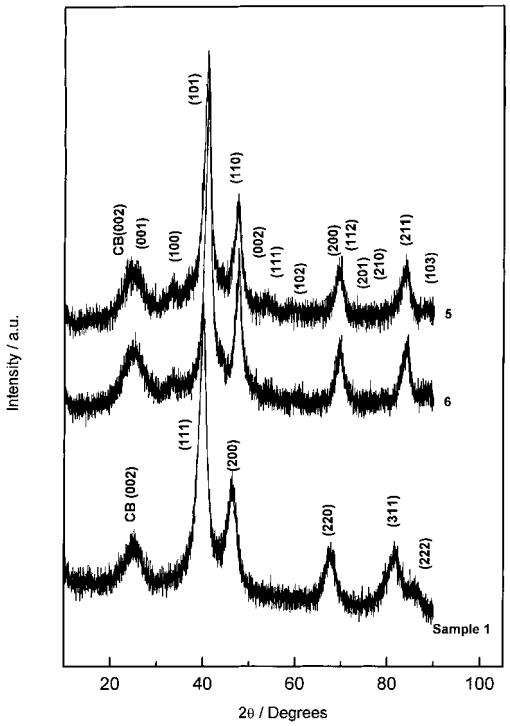

Fig. 2. Powder X-ray diffraction patterns of carbon-supported platinum-based ternary-alloy catalysts.

be akin to Pt_3M (M = Co, Cr, Ni) phases of the respective alloys [27, 28]. The metal content in two ternary-alloy catalysts, namely Pt–Co–Cr and Pt–Co–Ni, were found to be approximately 2:1:1 in atomic ratios.

The galvanostatic-polarization data for oxygen reduction at 70 °C and 2 bar oxygen pressure against a DHE are shown in Figure 3(a). The data suggest that the performance of the electrode containing 20 wt % Pt–Co/C catalyst is superior to that of the 20 wt % Pt/C electrode, as well as the other carbon-supported Pt-based binary and ternary-alloy catalysts. To examine the effect of temperature on polarization data of these electrodes, we also carried out galvanostatic-polarization studies at 90 °C and 2 bar oxygen pressure, as shown in Figure 3(b). An improvement of about 50 mV in the performance of the electrode containing Pt–Co/C catalyst was found over the entire range of polarization values. We also obtained galvanostatic-polarization

Table 1. Chemical compositions of various platinum-based carbon-supported catalysts as determined by EDAX

Sample	Catalyst compositions (Nominal)	Catalyst compositions (EDAX)
1	20 wt % Pt/C	–
2	20 wt % Pt–Co/C	61:39
3	20 wt % Pt–Cr/C	58:42
4	20 wt % Pt–Ni/C	60:40
5	20 wt % Pt–Co–Cr/C	51:22:27
6	20 wt % Pt–Co–Ni/C	57:23:20

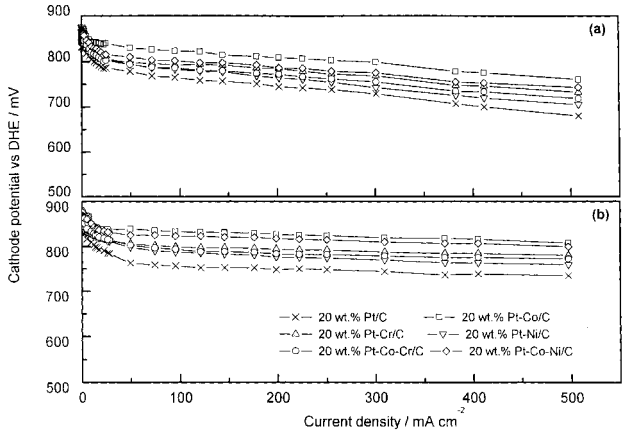

Fig. 3. Galvanostatic-polarization data for oxygen–reduction reaction on cathodes with various binary and ternary-alloy catalysts at (a) 70 °C, and (b) 90 °C both obtained at 2 bar oxygen pressure.

data for electrodes at ambient oxygen pressures both at 70 °C and 90 °C; the respective data are shown in Figure 4(a) and (b). Under all these conditions, the electrodes containing Pt–Co/C were found to exhibit the best performance.

For the electrodes used in this study, it is critical to get some measure of the active surface area of the catalysts participating in the oxygen–reduction reaction. As the electrodes are painted with Nafion® solution to provide the ionic contact with the platinum surface, it is possible for the extent of this contact to vary with the different catalyst formulations. This can have a large influence on the assessment of the merits of one catalyst compared to another. Platinum surface-areas from *in situ* cyclic voltammetry, which gives a good measure of it, are given in Table 2. Some variation in the Pt surface-areas for various catalyst formulations is evident. The current–voltage plots in Figures 3 and 4 have been corrected for available electrochemical surface areas and internal resistance to obtain Tafel slopes in order to best probe the kinetic effects at different catalyst

Table 2. Platinum surface-areas for various platinum-based carbon-supported catalysts as obtained from *in situ* cyclic voltammetry

Sample	Catalyst compositions (Nominal)	Pt surface-area /$m^2\ g^{-1}$
1	20 wt % Pt/C	103
2	20 wt % Pt–Co/C	82
3	20 wt % Pt–Cr/C	81
4	20 wt % Pt–Ni/C	72
5	20 wt % Pt–Co–Cr/C	84
6	20 wt % Pt–Co–Ni/C	97

surfaces. The respective Tafel slopes for Pt/C and Pt-Co/C electrodes for oxygen–reduction were found to be about 60 and 45 mV (decade)$^{-1}$. Accordingly, the respective exchange current-densities for the Pt and Pt–Co electrodes are estimated as 4.4×10^{-6} and 1.2×10^{-8} mA/cm^{-2}. The Pt–Co/C electrode seems to have poor electrocatalytic activity towards oxygen reduction in relation to Pt/C electrodes. Although, Pt–Co/C may be a poor electrocatalyst in terms of exchange current it appears to be electrocatalytically superior in relation to Pt/C at high overpotentials since the Tafel slope for Pt–Co/C electrodes has a relatively lower value [29]. The cell performance data, along with the constituent electrodes of the MEA comprising Pt–Ru/C and Pt/C cathodes operating at 70 °C and 2 bar oxygen pressure, are shown in Figure 5(a). Similar data for the cell operating at 90 °C and 2 bar oxygen pressure are shown in Figure 5(b). The galvanostatic-polarization data for the cell at 70 °C and 90 °C operating at ambient oxygen pressure are shown in Figure 6(a) and (b), respectively. Among these data, a maximum power density of 125 mW cm^{-2} is found for the cell operating at 90 °C with 2 bar oxygen pressure.

The cell performance data along with constituent electrodes of the MEA comprising Pt–Ru/C anode and Pt–Co/C cathode operating at 70 °C and 2 bar oxygen pressure, are shown in Figure 7(a). Similar data for the cell operating at 90 °C and 2 bar oxygen pressure are

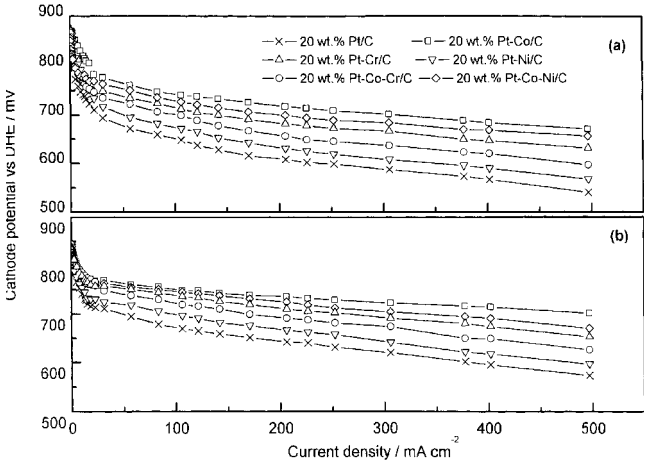

Fig. 4. Galvanostatic-polarization data for oxygen–reduction reaction on cathodes with various binary and ternary-alloy catalysts at (a) 70 °C, and (b) 90 °C both obtained at ambient oxygen pressure.

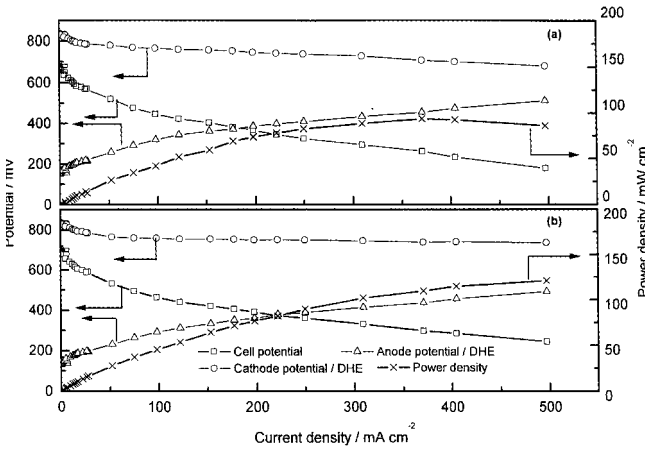

Fig. 5. Galvanostatic-polarization data for SPE–DMFCs employing 20 wt % Pt/C cathode catalyst obtained at (a) 70 °C, and (b) 90 °C both operating at 2 bar oxygen pressure.

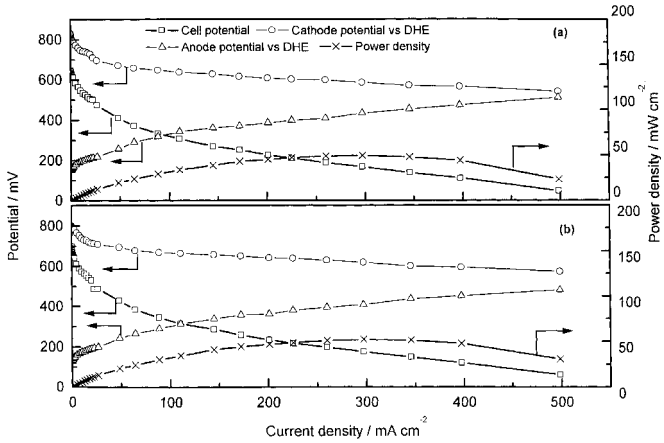

Fig. 6. Galvanostatic-polarization data for SPE–DMFCs employing 20 wt % Pt/C cathode catalyst obtained at (a) 70 °C, and (b) 90 °C both operating at ambient oxygen pressure.

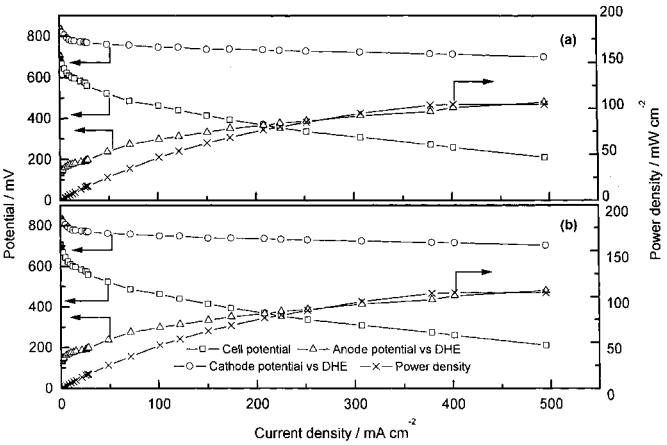

Fig. 8. Galvanostatic-polarization data for SPE–DMFC employing 20 wt % Pt–Co/C cathode catalyst obtained at (a) 70 °C, and (b) 90 °C both operating at ambient oxygen pressure.

shown in Figure 7(b). Relative to the cell operating at 70 °C and 2 bar oxygen pressure, an improvement of about 75 mV in the cell performance at its maximum power density of 160 mW cm^{-2} was noted while operating at 90 °C. This improvement may be attributed to the reduction in ohmic resistance of the cell due to increased conductivity of the Nafion™ membrane, as well as to an increase in the rates of both oxygen reduction and methanol oxidation at the cathode and anode sides of the MEA, respectively. The galvanostatic-polarization data for the cell at 70 °C and 90 °C, both operating at ambient oxygen pressure, are shown in Figure 8(a) and (b), respectively. Little change in the performance of the SPE–DMFC at 70 °C and 90 °C is seen under operation at ambient oxygen pressure.

A plausible explanation for the enhanced activity of Pt–Co/C for oxygen reduction is as follows. As pointed out by Yeager [30], oxygen reduction may take place by either a direct four-electron pathway or a peroxide route. The four-electron transfer has been reported with platinum phthalocyanine [31, 32]. On a metal or alloy–catalyst surface the peroxide pathway appears to be the dominant reaction mode. In this reaction, the oxygen molecule reacts with the surface by first accepting an electron from the catalyst as shown below.

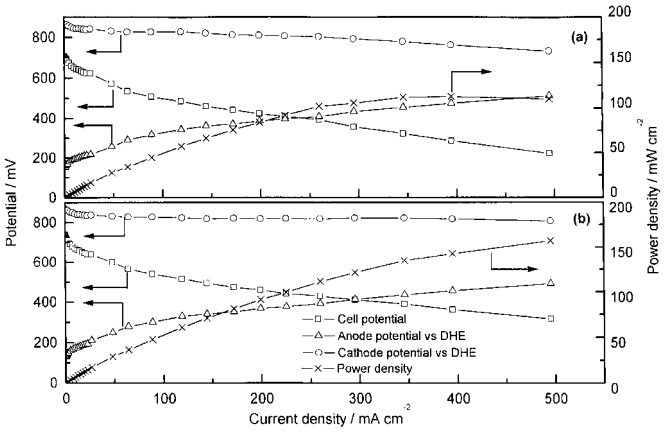

Fig. 7. Galvanostatic-polarization data for SPE–DMFC employing 20 wt % Pt–Co/C cathode catalyst obtained at (a) 70 °C and (b) 90 °C both operating at 2 bar oxygen pressure.

$$\mathrm{Pt\text{–}M + O_2 + e^- \longrightarrow Pt\text{–}M\text{–}O\text{–}O^-}$$

$$\xrightarrow{H^+_+e^-} \mathrm{Pt\text{–}M\text{–}O\text{–}OH^-} \quad (1)$$

$$\mathrm{Pt\text{–}M + O_2 \longleftrightarrow Pt\text{–}M^+\text{–}O\text{–}O^-}$$

$$\xleftrightarrow{H^+} \mathrm{Pt\text{–}M^{2+}\text{–}O\text{–}OH^-} \quad (2)$$

where Reaction 1 is electrochemical and Reaction 2 is purely chemical. However, in either case, the chemisorbed species is negatively charged. It is therefore electrostatically bound to the surface. If the reaction is chemical, the electrostatic component of the force between the chemisorbed species and the surface will depend on the applied voltage and the net intrinsic charge on the surface atom. In an element, the intrinsic charge is neutral and in a transition-metal alloy, like Pt–Co, the d-electron transfer from the constituent to the left in the periodic table makes this constituent effectively more positive as the empty d-states become the acceptors of the oxygen lone-pair electrons. For a given voltage, the d-electron transfer would make the constituent more attractive to the negatively charged species. In Pt–Co alloy, for example, an oxygen species will be more tightly bonded to the cobalt atom surface. In this alloy, therefore, cobalt acts as a promoter of Reaction 1. It is noteworthy that the active phase in the alloy is mainly composed of Pt sites and the Co-sites from the underlying layer exert their electronic effects as discussed by Toda et al. [33, 34]. Subsequently, two reaction pathways are available for the next critical step in the reduction process.

$$\mathrm{Pt\text{–}M\text{–}O\text{–}OH^- + H^+ + e^- \longrightarrow Pt\text{–}M\text{–}O^- + H_2O} \quad (3)$$

$$\mathrm{Pt\text{–}M\text{–}O\text{–}OH^- + H^+ \longleftrightarrow Pt\text{–}M + H_2O_2} \quad (4)$$

where Reaction 3 is electrochemical and Reaction 4 is chemical. In Pt–Co alloy, the more electropositive base-metal (M), namely Co, to which the oxygen species is attached, provides an electrostatic force that favours the desired electrochemical pathway relative to the chemical reaction. Thus, the electrochemical Reaction 3 is enhanced. The final steps in the electrochemical reduction reaction of oxygen are not rate limiting on either the elemental or alloy catalysts [35, 36].

4. Conclusions

This study shows that it is possible to substantially improve the performance of SPE–DMFCs by employing carbon-supported Pt–Co binary alloy as oxygen–reduction catalyst on the cathode side in place of carbon-supported platinum.

Acknowledgements

Financial support from the Department of Science and Technology, Government of India, is gratefully acknowledged.

References

1. S. Surampudi, S.R. Narayanan, E. Vamos, H. Frank, G. Halpert, A. LaConti, J. Kosek, G.K. Surya Prakash and G.A. Olah, *J. Power Sources* **47** (1994) 377.
2. M.K. Ravikumar and A.K. Shukla, *J. Electrochem. Soc.* **143** (1996) 2601.
3. X. Ren, M.S. Wilson and S. Gottesfeld, *J. Electrochem. Soc.* **143** (1996) L12.
4. L. Liu, C. Pu, R. Viswanathan, Q. Fan, R. Liu and E. S. Smotkin, *Electrochim. Acta* **43** (1998) 3657.
5. A.S. Aricò, P. Creti, P.L. Antonucci and V. Antonucci, *Electrochem. Solid State Lett.* **1** (1998) 4.
6. A.K. Shukla, M.K. Ravikumar and K.S. Gandhi, *J. Solid State Elctrochem.* **2** (1998) 117.
7. S. Wasmus and A. Küver, *J. Electroanal. Chem.* **461** (1999) 14.
8. V. Trapp, P. Christensen and A. Hamnett, *J. Chem. Soc. Faraday Trans.* **21** (1996) 4311.
9. R.W. Reeve, P.A. Christensen, A. Hamnett, S.A. Haydock and S.C. Roy, *J. Electrochem. Soc.* **145** (1998) 3463.
10. V. Jalan and E.J. Taylor, *J. Electrochem. Soc.* **130** (1983) 2299.
11. J.T. Glass, G.L. Cahen, Jr., G.E. Stoner and E.J. Taylor, *J. Electrochem. Soc.* **134** (1987) 58.
12. K.A. Daube, M.T. Paffet, S. Gottesfeld and C.T. Campbell, *J. Vac. Sci. Technol.* **A4** (1986) 1617.
13. M. Watanabe, K. Tsurumi, T. Mizukami, T. Nakamura and P. Stonehart, *J. Electrochem. Soc.* **141** (1994) 2659.
14. P. Stonehart, *Ber. Bunsenges. Phys. Chem.* **94** (1990) 913.
15. W. Roh, J. Cho and H. Kim, *J. Appl. Electrochem.* **26** (1996) 623.
16. K.T. Kim, J.T. Hwang, Y.G. Kim and J.S. Chung, *J. Electrochem. Soc.* **140** (1993) 31.
17. B.C. Beard and P.N. Ross, Jr., *J. Electrochem. Soc.* **137** (1990) 3368.
18. F.J. Luckzak, L.J. Buchanan and G.A. Hards, *US Patent* 5 013 618 (1991).
19. L. Keck, J. Buchanan and G.A. Hards, *US Patent* 5 068 161 (1991).
20. D.A. Landsman and F.J. Luczack, *US Patent* 4 316 944 (1982).
21. H.G. Petrow and R.J. Allen, *US Patent* 3 992 331 (1976).
22. S. Mukerjee and S. Srinivasan, *J. Electroanal. Chem.* **357** (1993) 201.
23. S. Mukerjee, S. Srinivasan, M.P. Soriaga and J. McBreen, *J. Electrochem. Soc.* **142** (1995) 1409.
24. G. Thamizhmani and G.A. Capuano, *J. Electrochem. Soc.* **141** (1994) 968.
25. T. Beigler, D.A.J. Rand and R. Woods, *J. Electroanal. Chem.* **29** (1971) 269.
26. P. Villars, A. Prince and H. Okamoto (Eds), 'Handbook of Ternary Alloy Phase Diagrams', Vols 6–7, ASM International, The Materials Information Society (1995).
27. A. Freund, J. Lang, T. Lehman and K.A. Starz, *Catal. Today* **27** (1996) 279.
28. T.B. Massalski (Ed), '*Binary Alloy Phase Diagrams*', Vols 2–3, 2nd edn ASM International, The Materials Information Society (1990).
29. S. Trasatti and G. Lodi, *in* S. Trasatti (Ed), *Electrodes of conductive metallic oxides*, Part-B, Elsevier, Amsterdam, (1981), p. 38.
30. E. Yeager, *J. Mol. Catal.* **5** (1986) 38.
31. C. Paliteiro, A. Hamnett and J.B. Goodenough, *J. Electroanal. Chem.* **160** (1984) 359.
32. A.K. Shukla, C. Paliteiro, R. Manoharan, A. Hamnett and J.B. Goodenough, *J. Appl. Electrochem.* **19** (1989) 105.
33. T. Toda, H. Igarashi and M. Wantanabe, *J. Electroanal. Chem.* **460** (1999) 258.
34. T. Toda, H. Igarashi, H. Uchida and M. Wantanabe, *J. Electrochem. Soc.* **146** (1999) 3750.
35. K. Kordesch and G. Simader, '*Fuel Cells and their Applications*' VCH, Weinheim, (1996), p. 36.
36. J.B. Goodenough, R. Manoharan, A.K. Shukla and K.V. Ramesh, *Chem. Mater.* **1** (1998) 39.